ARTICLE

OBC
www.rsc.org/obc

Structural and mechanistic studies on anthocyanidin synthase catalysed oxidation of flavanone substrates: the effect of C-2 stereochemistry on product selectivity and mechanism

Richard W. D. Welford,† Ian J. Clifton, Jonathan J. Turnbull, Stuart C. Wilson and Christopher J. Schofield*

Chemical Research Laboratory, Department of Chemistry and Oxford Centre for Molecular Sciences, Mansfield Rd, Oxford, UK OX1 3TA. E-mail: christopher.schofield@chem.ox.ac.uk; Fax: +44 (0)1865 275674; Tel: +44 (0)1865 275625

Received 20th May 2005, Accepted 19th July 2005
First published as an Advance Article on the web 1st August 2005

During the biosynthesis of the tricyclic flavonoid natural products in plants, oxidative modifications to the central C-ring are catalysed by Fe(II) and 2-oxoglutarate dependent oxygenases. The reactions catalysed by three of these enzymes; flavone synthase I, flavonol synthase and anthocyanidin synthase (ANS), are formally desaturations. In comparison, flavanone 3β-hydroxylase catalyses hydroxylation at the C-3 *pro-R* position of 2*S*-naringenin. Incubation of ANS with the unnatural substrate (±)-naringenin results in predominantly C-3 hydroxylation to give *cis*-dihydrokaempferol as the major product; *trans*-dihydrokaempferol and the desaturation product, apigenin are also observed. Labelling studies have demonstrated that some of the formal desaturation reactions catalysed by ANS proceed *via* initial C-3 hydroxylation followed by dehydration at the active site. We describe analyses of the reaction of ANS with 2*S*- and 2*R*-naringenin substrates, including the anaerobic crystal structure of an ANS–Fe–2-oxoglutarate–naringenin complex. Together the results reveal that for the 'natural' C-2 stereochemistry of 2*S*-naringenin, C-3 hydroxylation predominates (>9 : 1) over desaturation, probably due to the inaccessibility of the C-2 hydrogen to the iron centre. For the 2*R*-naringenin substrate, desaturation is significantly increased relative to C-3 hydroxylation (*ca.* 1 : 1); this is probably a result of both the C-3 *pro-S* and C-2 hydrogen atoms being accessible to the reactive oxidising intermediate in this substrate. In contrast to the hydroxylation–elimination desaturation mechanism for some ANS substrates, the results imply that the ANS catalysed desaturation of 2*R*-naringenin to form apigenin proceeds with a *syn*-arrangement of eliminated hydrogen atoms and *not via* an oxygenated (gem-diol) flavonoid intermediate. Thus, by utilising flavonoid substrates with different C-2 stereochemistries, the balance between C-3 hydroxylation or C-2, C-3 desaturation mechanisms can be altered.

Introduction

The flavonoids are polyphenolic natural products found in plants and some micro-organisms. They play roles in pigmentation, protection against UV photodamage, can act as signalling molecules, and have been reported to possess a variety of biomedicinal properties, including anti-malarial, anti-oxidant and anti-tumour activities.[1]

One of the key sites for structural diversification of flavonoids is the central C-ring. Modifications to this ring are brought about by oxygenases and reductases (Fig. 1A).[2,3] Four of the oxygenases known to catalyse modification of the C-ring in plants are Fe(II) and 2-oxoglutarate dependent oxygenases: flavone synthase I,[4] flavanone 3β-hydroxylase,[5] flavonol synthase[6,7] and anthocyanidin synthase (ANS)[8,9] (Fig. 1A).

The non-haem Fe(II), 2-oxoglutarate dependent oxygenase family of enzymes utilise a 2-oxoglutarate **1** (2OG) co-substrate to effect a 2 electron oxidation of their substrate (Fig. 1B).[10,11] Most commonly, substrate oxidation involves hydroxylation, though some members of the family catalyse other oxidative reactions such as desaturation or ring expansion. The 2OG **1** co-substrate is decarboxylated to give succinate **2** containing one oxygen atom derived from dioxygen; the other dioxygen atom is typically incorporated into the product in the case of hydroxylation reactions. The oxidising intermediate effecting hydroxylation is thought to be a ferryl species (Fe^{IV}=O) (Fig. 1B). This intermediate has recently been characterised spectroscopically in the reaction cycle of the enzyme taurine dioxygenase.[12–14]

During flavonoid biosynthesis, flavone synthase I catalyses desaturation of 2*S*-naringenin **3** to give apigenin **4** (Fig. 1A). It is thought that this reaction proceeds by abstraction of the C-3 *pro-R* and C-2 hydrogen atoms that are in a *syn*-facial arrangement.[4,15] Flavanone 3β-hydroxylase catalyses hydroxylation of the *pro-R* hydrogen at C-3 of 2*S*-naringenin **3** producing 2*R*,3*R*-*trans*-dihydrokaempferol **5** (2*R*,3*R*-*trans*-DHK). Flavonol synthase catalyses a formal desaturation of 2*R*,3*R*-*trans*-dihydroflavonols (*e.g.* **5**) to form flavonols. However, the results from incubations of flavonol synthase and ANS with unnatural flavanone (*e.g.* 2*S*-naringenin **3**) substrates have provided evidence that both these enzymes catalyse C-3 hydroxylation of, at least, some dihydroflavonol (*e.g.* **5**) substrates, followed by dehydration, rather than direct desaturation (Fig. 2A).[6,7,16]

There is uncertainty about the exact *in vivo* role of ANS.[17] ANS was originally thought to catalyse conversion of 2*R*,3*S*,4*S*-*cis*-leucoanthocyanidins (*e.g.* **6**) to anthocyanidins (*e.g.* **7**).[8] However, *in vitro* incubations of purified ANS from *Arabidopsis thaliana* (*A. thaliana*) with 2*R*,3*S*,4*S*-*cis*-leucocyanidin **6** (2*R*,3*S*,4*S*-*cis*-LCD) produces cyanidin **7** as only a minor product, with the major product, quercetin **8** arising from 4 electron oxidation, a process that requires two catalytic cycles (Fig. 2B).[17] ANS can also catalyse the oxidation of other flavonoid substrates, often producing a mixture of products. Incubation of ANS with leucocyanidin of the 'unnatural' stereochemistry (2*R*,3*S*,4*R*-*trans*-LCD, the C-4 epimer of 2*R*,3*S*,4*S*-*cis*-LCD **6**) leads to a mixture of both 2 and 4 electron oxidation products;[9,16,17] quercetin **8** (30%) and the thermodynamically less stable *cis*-diastereoisomer of the dihydroflavonol, dihydroquercetin (DHQ) (55% of products) predominate, with the latter being produced as a single enantiomer. ANS also catalyses

† *Current address:* UC Berkeley, Department of Chemistry, Berkeley, CA 94720, USA.

DOI: 10.1039/b507153d

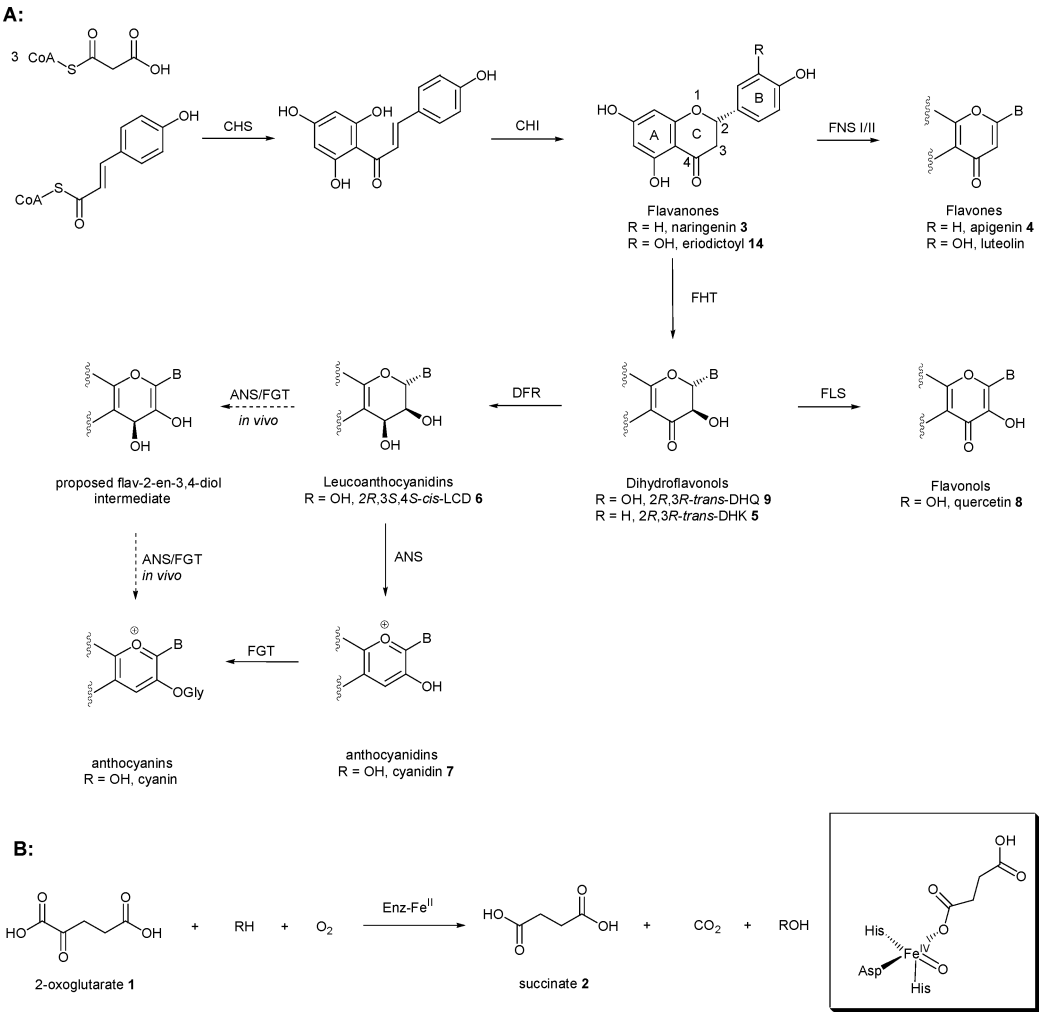

Fig. 1 **A** Current proposals for the flavonoid biosynthetic pathway. Flavonoid nomenclature is indicated on the flavanone (2*S*-naringenin **3**) structure. Under each structure a flavonoid class name is given and underneath that, the compound name for different hydroxylation patterns is given. Subsequent to 2*S*-naringenin **3**, 'B' is used to represent the B-ring and the A-ring is not shown. This representation is also used in subsequent figures. For the steps after formation of the leucoanthocyanidins (*e.g.* **6**), the dotted lines represent the originally proposed pathway, while the solid lines indicate a new proposal based on recent *in vitro* evidence.[17] CHS = chalcone synthase, CHI = chalcone isomerase, FNS I/II = flavone synthase I or II, FHT = flavanone 3β-hydroxylase, FLS = flavonol synthase, DFR = dihydroflavonol reductase, ANS = anthocyanidin synthase, FGT = flavonol glycosyl transferase. **B** Hydroxylation reaction of a Fe(II), 2OG dependent oxygenase; the Fe^{IV}=O intermediate is shown boxed.

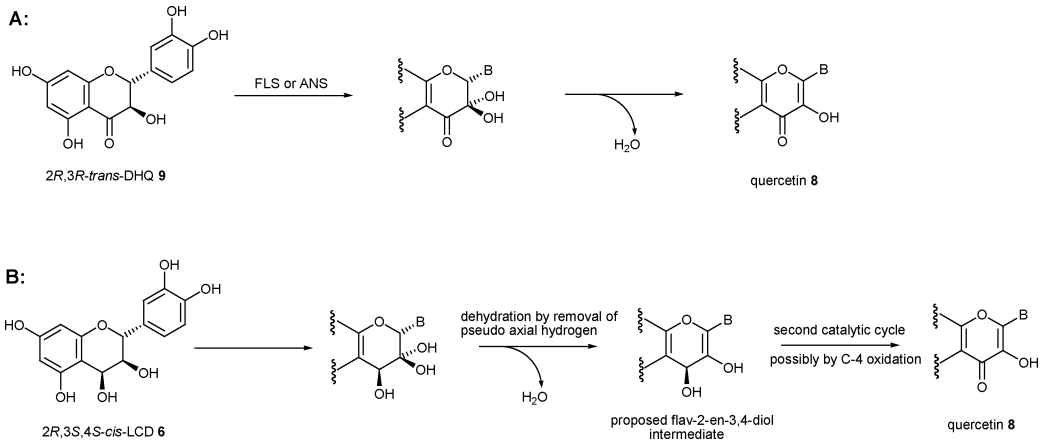

Fig. 2 **A** Outline mechanism for C-3 hydroxylation and dehydration mechanism for desaturation of 2*R*,3*R*-*trans*-DHQ **9** by ANS or flavonol synthase to form quercetin **8**.[23] FLS = flavonol synthase, ANS = anthocyanidin synthase. **B** Proposed mechanism for formation of quercetin **8** from 2*R*,3*S*,4*S*-*cis*-LCD **6** *via* an initial C-3 oxidation step—details are given in Turnbull *et al.*[17,23]; a mechanism proceeding *via* oxidation at C-4 cannot be ruled out.

Table 1 Percentage of total of products formed by ANS incubations with racemic naringenin **3/13** and racemic eriodictyol **14** as analysed by HPLC. Note that *cis*-**10** and *trans*-DHK **5/11** were not resolved under the conditions used, see Table 3 for the ratio of *cis* and *trans*. DHK = dihydrokaempferol, DHQ = dihydroquercetin

Substrate	*trans*-Dihydroflavonol (%)	*cis*-Dihydroflavonol (%)	Flavone (%)	Flavonol (%)
(±)-Naringenin **3/13**	60 (DHK)		33 (Apigenin)	7 (Kaempferol)
(±)-Eriodictyol **14**	29 (DHQ)	61 (DHQ)	10 (Luteolin)	<1 (Quercetin)

desaturation of 2*R*,3*R*-*trans*-DHQ **9**; a reaction catalysed *in vivo* by flavonol synthase (Fig. 1A).[9] The crystal structures of three ANS complexes have been solved: ANS–2OG, with the unnatural 2*R*,3*R*-*trans*-DHQ **9** substrate ANS–Fe–2OG–DHQ_2 and following exposure of the 2*R*,3*R*-*trans*-DHQ **9** complex crystals to dioxygen, a ANS–Fe–succinate–quercetin–DHQ product complex.[18]

In vitro, both ANS and flavonol synthase have been reported to catalyse oxidation of 2*S*-naringenin **3**, the natural substrate of flavone synthase I and flavanone 3β-hydroxylase. We have communicated that incubation of ANS with the unnatural substrate (±)-naringenin **3/13** gives the C-3 hydroxylation product *cis*-DHK **10** as a single enantiomer as the major species (ee >70%),[16] with lower levels of *trans*-DHK **5/11** (of undetermined enantiomeric purity) and kaempferol **12** also being observed. Flavonol synthase from *A. thaliana* has also been shown to react with both enantiomers of the unnatural substrate naringenin.[6] It converts the 'natural' C-2 enantiomer 2*S*-naringenin **3** to 2*R*,3*S*-*cis*-DHK **10**, 2*S*,3*S*-*trans*-DHK **11** and kaempferol **12**. Similarly flavonol synthase from *Citrus unshiu* has been shown to convert 2*S*-naringenin **3** to kaempferol **12**, in a process that was thought to be due to two catalytic cycles[7] with the first converting 2*S*-naringenin **3** to 2*R*,3*R*-*trans*-DHK **5**, with this product then being desaturated enzymatically to kaempferol **12**. Flavonol synthase from both *Citrus unshiu*[7] and *A. thaliana*[6] has been shown to convert 2*R*-naringenin **13** to 2*S*,3*S*-*trans*-DHK **11**, resulting from hydroxylation of the C-3 *pro*-*S* hydrogen atom.

Members of the family of non-haem Fe(II), 2OG dependent oxygenases are known to catalyse different types of oxidation reactions with different substrates. For example, clavaminic acid synthase catalyses three reactions comprising hydroxylation, oxidative ring expansion and desaturation processes in the biosynthesis of clavulanic acid.[19–21] Further, the structurally related Fe(II) dependent oxidase isopenicillin *N*-synthase has a diverse substrate and reaction selectivity. With different unnatural substrates it has been observed to catalyse hydroxylation, ring expansion, desaturation and epoxidation reactions.[22] Understanding the factors that determine which type of oxidative reaction a non-haem Fe(II) oxygenase carries out is a challenge that may bring about a better understanding of these catalysts. This information may also be used in the design of successful synthetic catalysts that mimic enzymes.

Here we describe the *in vitro* products of assays of ANS with 2*R*-**13** and 2*S*-naringenin **3**, a crystal structure of an ANS–Fe–2OG–naringenin complex and the activity of mutant forms of ANS. The results demonstrate that in the case of naringenin substrates, the product selectivity of ANS is dependent upon the C-2 stereochemistry and that the balance between desaturation and hydroxylation relates to the accessibility of the C-2 hydrogen atom to the reactive oxidising intermediate.

Results

Assays

Initially, the product ratios from incubations of ANS (*A. thaliana*) with racemic mixtures of unnatural flavanone substrates, (±)-eriodictyol **14** and (±)-naringenin **3/13**, which have differing B-ring hydroxylation patterns, were analysed by HPLC (eriodictyol **14** has the same hydroxylation pattern as naringenin **3** but with an additional 3′ hydroxyl group). (±)-Eriodictyol **14** was not an efficient substrate of ANS (with *ca.* 30% of the turnover of (±)-naringenin **3/13** being observed under standard conditions). The HPLC analyses indicated that in both cases, the hydroxylated dihydroflavonol product(s) predominate (*e.g.* DHK **5/10** from naringenin), with some desaturation product, flavone (*e.g.* apigenin **4** from naringenin) also being observed (Table 1). The flavone product made up a greater proportion of the overall product in assays with (±)-naringenin **3/13** than with (±)-eriodictyol **14**. These observations imply that the balance between destauration and hydroxylation is in part determined by the hydroxylation pattern on the flavonoid B-ring.

Enantiomerically enriched naringenin substrates (2*S*-**3** and 2*R*-**13**) were prepared by the enzymatic cleavage of the appropriate 7-*O*-rhamnose of 2*S*- and 2*R*-naringin using commercially available naringinase from *Penicillium decumbens*. The chiral purity of the naringenin products (**3** and **13**) could not be measured directly either by chiral-NMR (the lanthanide chiral shift method developed detects dihydroflavonol enantiomers[16,17] at the C-3 position) or chiral-HPLC (which was unable to resolve the enantiomers under the conditions tested with a ChiraSpher® NT column). However, subsequent HPLC analysis revealed significantly differing product distributions obtained from incubations of ANS with the racemic **3/13** and the chirally pure (**3** and **13**) naringenin substrates (Table 2). These results infer that the chiral integrity of the naringin had largely been unaffected under the conditions required for cleavage of its glycosidic bond.

Analyses measuring the production of $^{14}CO_2$ from 1-[^{14}C]-2OG co-substrate has indicated that both 2*S*-**3** and 2*R*-naringenin **13** are substrates of ANS.[23] The similarity in the specific activity values as measured by $^{14}CO_2$ formation using either 2*R*-**13** or 2*S*-naringenin **3** enantiomers was in marked contrast to those observed on incubations of ANS with racemic and chirally pure LCD and DHQ. In the cases of both LCD and DHQ, ANS was much more active with the chirally pure substrates of the natural stereochemistry (2*R*,3*S*,4*S*-**6** (LCD), and 2*R*,3*R*-**9** (DHQ) respectively). Thus the presence of a C-3 hydroxyl group, as in leucoanthocyanidins (**6**) and dihydroflavonols (**9**), enables ANS to be selective for substrates with a particular C-2 stereochemistry.

HPLC analyses revealed significantly differing product distributions in incubations of ANS with the racemic (**3/13**), 2*S*-**3** and 2*R*-naringenin **13** substrates (Table 2, Figs. 3 and 4). For incubation with (±)-naringenin **3/13** the major product observed was DHK. With the 'natural' C-2 stereochemistry of 2*S*-naringenin **3**, the major product (~74% of isolated products as analysed by HPLC) was also DHK (**5/10/11**), with only minor amounts of the desaturated product, apigenin **4** (~1%), being formed. However, with the 'unnatural' stereochemistry of 2*R*-naringenin **13**, apigenin **4** was formed in significant quantities (~44%). Note in the racemic mixture **3/13**, the *S*-isomer **3** is likely to be selectively oxidised, hence rationalising

Table 2 Ratios of products formed from ANS incubations with racemic **3/13**, 2*S*-**3** and 2*R*-**13** naringenin as analysed by HPLC

Substrate	DHK	Apigenin	Kaempferol
(±)-Naringenin **3/13**	60	33	7
2*S*-Naringenin **3**	74	1	25
2*R*-Naringenin **13**	50	44	6

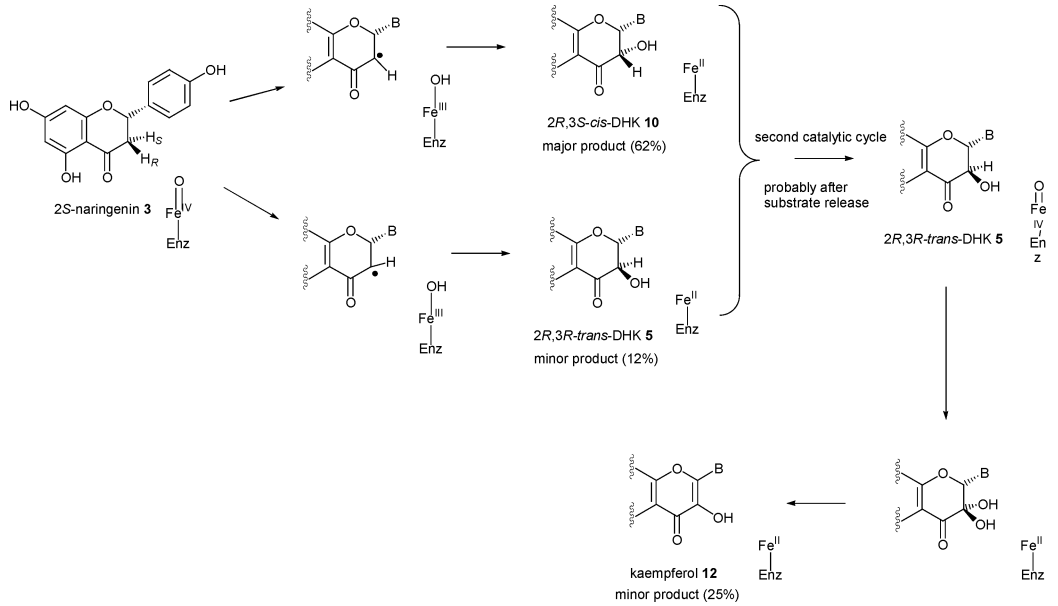

Fig. 3 The reaction of ANS with the 2*S*-naringenin **3** substrate showing pathways for formation of *cis*-DHK **10**, *trans*-DHK **5/11** and kaempferol **12** products.

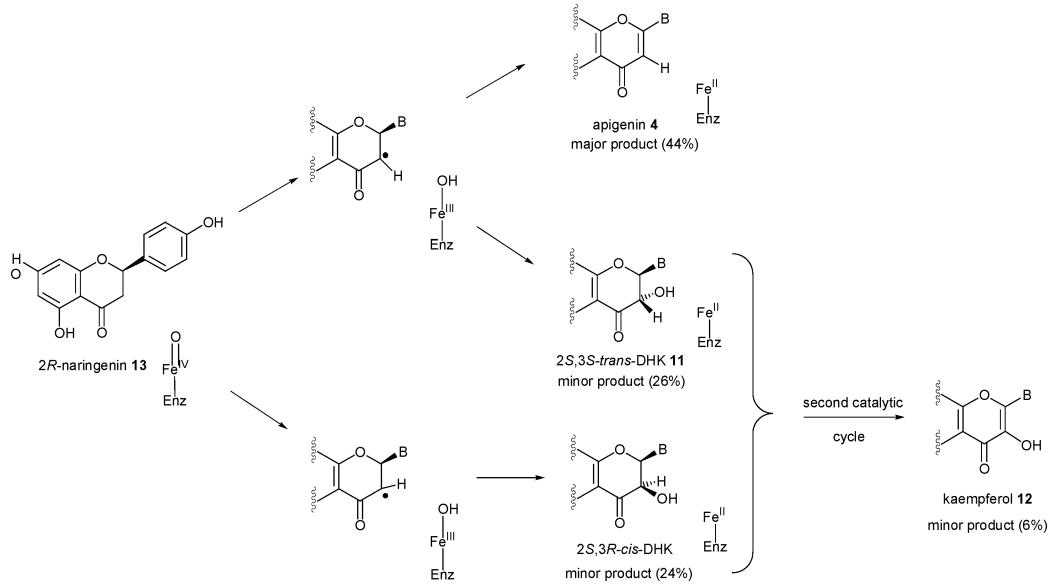

Fig. 4 The reaction of ANS with the 2*R*-naringenin **13** substrate showing pathways for formation of *cis*-DHK **10**, *trans*-DHK **5/11**, apigenin **4** and kaempferol **12** products.

the similar results obtained for the racemic and *S*-isomer. These results imply that a 2*R*-C-2 stereochemistry coupled to the presence of a *syn* hydrogen at C-3 is required for a *direct* desaturation of flavanone (*e.g.* **3**) substrates by ANS.

After isolation of the DHK (**5/10/11**) produced from *in vitro* assays of ANS incubated with racemic **3/13**, 2*S*-naringenin **3** and 2*R*-naringenin **13**, chiral HPLC (using a ChiraSpher® NT chiral column) was used to separate the *trans*-**5/11** and *cis*-DHK **10** diastereomers (Table 3). Resolution of the enantiomers of both *trans*-**5/11** and *cis*-DHK **10** was not possible under the conditions tested. HPLC analyses of incubation mixtures were carried out immediately after quenching, so as to minimise conversion of the *cis*-isomers **10** to the more thermodynamically stable *trans*-isomers **5/11**. The thermodynamic ratio of *trans*-**11** : *cis*-**10** DHK, is *ca.* 9 : 1, with isomerisation occurring *via* C-4′ hydroxyl assisted opening of the C-ring.[16,24] For incubations of (±)-naringenin **3/13** and 2*S*-naringenin **3** with ANS, *cis*-DHK **10** was produced in excess to the thermodynamically more stable *trans* diastereomer (**5** and **11**) (*ca.* 4 : 1 and 5.2 : 1, respectively). For the 2*R*-naringenin **13** substrate of ANS, the diastereoselectivity of DHK formation was much reduced with similar amounts of both *cis* (**10** and/or enantiomer) and *trans*-DHK **5/11** products being produced.

Table 3 Ratios of *trans*- and *cis*-DHK production of ANS incubations with racemic **3/13**, 2*S*-**3** and 2*R*-**13** naringenin as determined by HPLC

Substrate	*trans*-DHK	*cis*-DHK
(±)-Naringenin **3/13**	1	4.0
2*S*-Naringenin **3**	1	5.2
2*R*-Naringenin **13**	1.1	1

The flavonoid products from an incubation of ANS with (±)-naringenin **3/13** were separated from the co-factor, co-products and enzymes in the assay mixture by solid phase extraction[17,23] and analysed by ^{1}H NMR with minimal exposure to solvent and elevated temperature (Fig. 5). The ^{1}H NMR analyses confirmed the assignment of *cis*-DHK **10**, *trans*-DHK **5/11** and apigenin **4** products, though insufficient material of the minor product kaempferol **12** was present to obtain a definitive spectrum. The ratio of *cis*-**10** to *trans*-DHK **5/11** observed (4 : 1 by integration of the C-2 proton resonance) was similar to that observed by

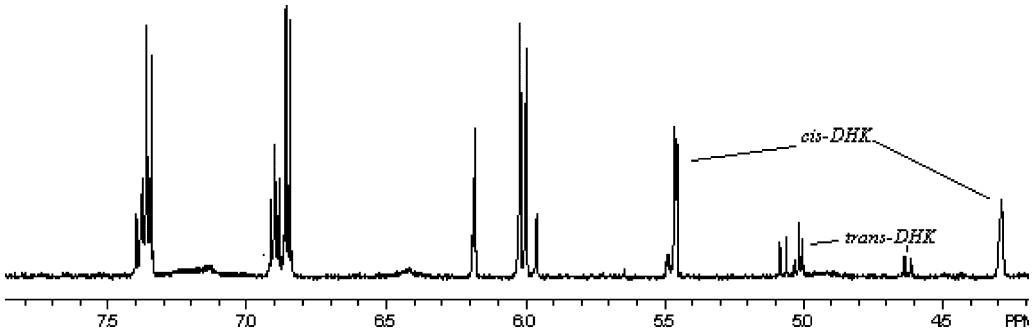

Fig. 5 ^{1}H NMR spectrum of *cis* **10** and *trans*-dihydrokaempferol **5/11** purified from an incubation of ANS with (±)-naringenin **3/13**.

HPLC. Using NMR spectroscopy, the lanthanide chiral shift reagent europium tris[3-heptafluoropropylhydroxymethylene)-(+)-camphorate (Eu(hfc)$_3$) can be used to distinguish the enantiomers of dihydroflavonols, *e.g.* DHQ (**9** and enantiomer) (Fig. 6).[16] Addition of increasing amounts of Eu(hfc)$_3$ did not cause any splitting of the C-5 hydroxyl proton resonance at δ_H 11.75, indicating that *cis*-DHK **10** was formed, at least predominantly, as a single enantiomer (Fig. 7).[16] The intensity of the *trans*-DHK resonance was too small to determine whether any splitting occurred on addition of the chiral shift reagent; some or all of the *trans*-DHK observed may thus be formed by isomerisation of *cis*-DHK **10**. In comparison for a standard of (±)-*cis*/*trans*-DHQ (**9** and stereoisomers) the C-5 hydroxyl proton resonance of both diastereomers was split on addition of between 0.25 and 1 equivalent of Eu(hfc)$_3$ (Fig. 6).

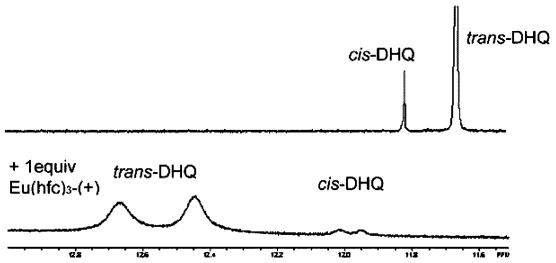

Fig. 6 Effect of the lanthanide chiral shift reagent Eu(hfc)$_3$-(+) on the NMR spectrum of a thermodynamic mixture of (±)-*trans*-dihydroquercetin (**9** and enantiomer) and (±)-*cis*-dihydroquercetin. Note that if pure (+)-*trans*-dihydroquercetin **9** was added to the mixture, only one of the peaks observed in the lower spectrum increased in magnitude.

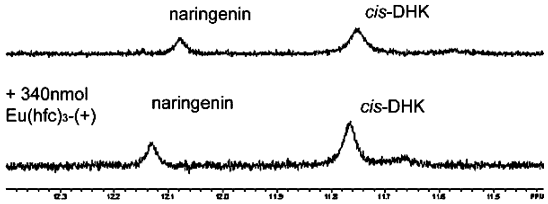

Fig. 7 Effect of lanthanide chiral shift reagent Eu(hfc)$_3$-(+) on the NMR spectrum of *cis*-**10** and *trans*-dihydrokaempferol **5/11** purified from an incubation of (±)-naringenin **3/13**.

To investigate the orientation of naringenin in the ANS active site, co-crystallisation of ANS with (±)-naringenin **3/13** was carried out (Figs. 8–10). In the ANS–Fe–2OG–DHQ–MES crystal structure, two molecules of DHQ **9** were observed to be complexed to the active site. The DHQ molecule in place to be oxidised (*i.e.* that closest to the iron) was the 2*R*,3*R*-*trans*-**9** stereoisomer; its C-3 hydrogen was in a position where it could potentially be oxidised, with relatively little movement, by an iron centred ferryl species (Fe^{IV}=O), while the C-2 hydrogen was more distant and pointed away from the iron centre.[18] This observation is consistent with a mechanism involving oxygenation at C-3 during desaturation of 2*R*,3*R*-*trans*-DHQ **9** by ANS. A more direct desaturation (either concerted or non-concerted) process appeared much less likely. In addition, a second molecule of DHQ substrate was present in the active site of this crystal structure (assigned as the 2*S*,3*S*-*trans* enantiomer), along with a molecule of the 2-[*N*-morpholino]ethanesulfonic acid (MES) buffer present in the crystallisation solution.

The overall arrangement of the active site residues in the ANS–Fe(II)–2OG–naringenin structure is very similar to that observed in the previously described structures of ANS–Fe(II)–2OG–DHQ$_2$–MES and ANS–Fe(II)–succinate–quercetin[18] (RMS of 0.42 Å to 1gp5). A single molecule of 2*S*-naringenin **3** is complexed in the active site in a similar manner to DHQ-1 **9** in the ANS–Fe(II)–2OG–DHQ structure. A 2*S*-naringenin **3** substrate molecule was modelled into the electron density, although the lower resolution (2.3 Å) of the ANS–Fe(II)–2OG–naringenin meant that (partial) occupancy by the 2*R*-naringenin **13** could not be ruled out.

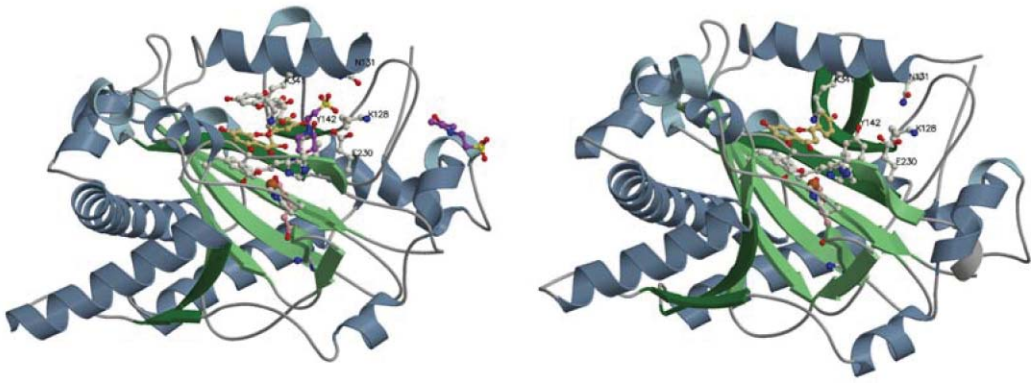

Fig. 8 Overall view of ANS–Fe(II)–2OG–DHQ$_2$–MES. Left: PDB structure 1gp5 containing 2OG (pink), two molecules of MES (purple) and two molecules of dihydroquercetin (DHQ). DHQ-1 and DHQ-2 are 2*R*,3*R*-*trans* (buff) and 2*S*,3*S*-*trans* (grey) stereochemistries respectively. Right: the structure described here, with 2OG (pink) and one molecule of 2*S*-naringenin (buff).

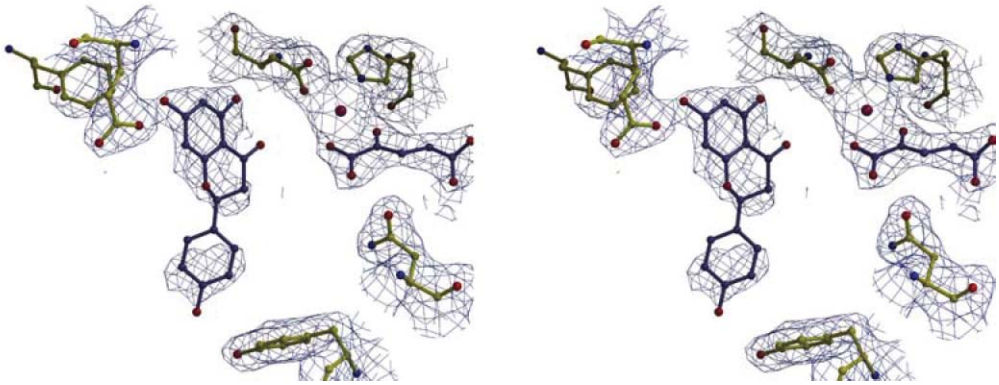

Fig. 9 Stereo diagram of the ANS active site with $2mF_o$-DF_c electron density map plotted at a contour level of 1σ.

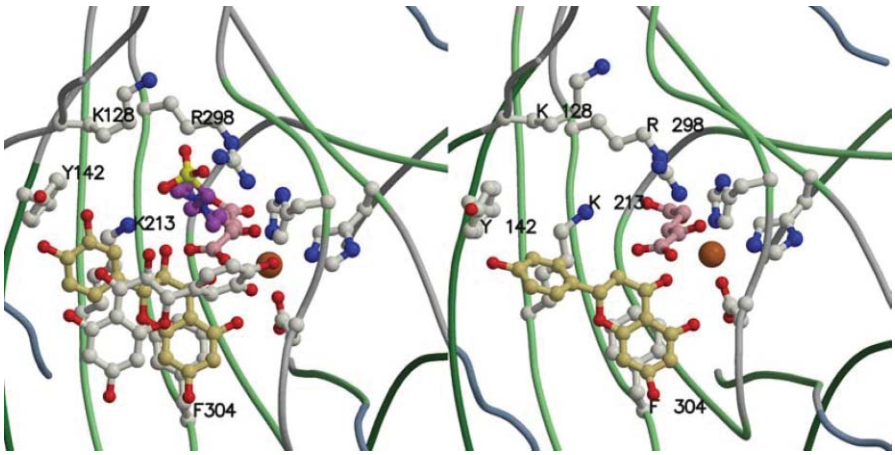

Fig. 10 The active site of ANS depicted using the same colour scheme as Fig. 8. Left: the 2*R*,3*R*-*trans*-DHQ **9** structure. Right: the 2*S*-naringenin **3** structure.

There are some significant changes between the active sites of the ANS–Fe(II)–2OG–DHQ_2–MES and ANS–Fe(II)–2OG–naringenin–MES structures. In the 2*S*-naringenin **3** structure, there was no density in the active site corresponding to a second molecule of naringenin equivalent to 'DHQ-2′ in the ANS–Fe(II)–2OG–DHQ_2–MES structure. The lower concentration of substrate present in the co-crystallisation of ANS with naringenin **3/13** compared to DHQ (**9** and enantiomer), (final concentrations of 2.5 mM and 10 mM respectively) may in part, have resulted in this; however, the 2.5 mM solution of naringenin **3/13** used still represents an eight-fold excess of naringenin **3/13** relative to ANS.

In the ANS–Fe(II)–2OG–DHQ_2–MES structure, the 3′-hydroxyl group of the second DHQ (enantiomer of **9**) molecule is in position to hydrogen bond with the C-5 hydroxyl group of the A-ring of DHQ-1 **9** and the main chain carbonyl of Thr233. The absence of a 3′-hydroxyl group in the naringenin **3/13** substrate may not allow efficient binding in an analogous manner.

An assay monitoring the decarboxylation of a 1-[^{14}C]-2OG co-substrate was used to investigate the effect of varying the initial concentration of different flavonoid substrates on the rate of ANS reaction (Fig. 11). For both (±)-naringenin **3/13** and (±)-*trans*-DHQ (**9** and enantiomer) substrates the initial rate increased to a maximum at approximately 800 μM. After this the rate began to decrease. This demonstrates that substrate inhibition occurs for both (±)-naringenin **3/13** and (±)-*trans*-DHQ **9**, despite the observation that two molecules of flavonoid were observed in the crystallographic analysis of the active site only in the latter case. The precise mechanism(s) of substrate inhibition is uncertain. However, it seems reasonable to propose that binding at the second substrate binding site, observed with DHQ (**9** and enantiomer), will inhibit product release and hence reduces the efficiency of enzymatic turnover, at least for

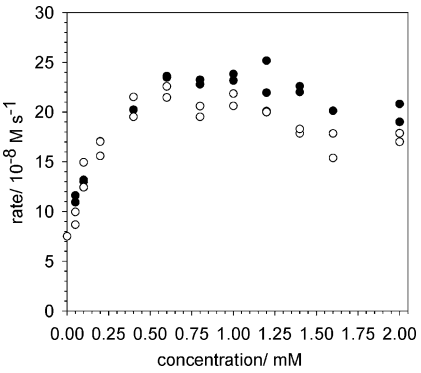

Fig. 11 The effect of different concentrations of flavonoid substrate on the rate of decarboxylation of the 2OG **1** co-substrate. Note that the rate is non-zero in the absence of flavonoid substrate due to the substrate uncoupled reaction of 2OG. Black circles with a (±)-*trans*-DHQ (**9** and enantiomer) substrate; open circles with a (±)-naringenin **3/13** substrate.

substrates with 3′- or 3′,5′-hydroxyl groups. It is possible that binding of a second substrate (flavonoid) represents a method for obtaining a degree of selectivity related to the hydroxylation pattern of the B-ring (note that the B-ring hydroxylation pattern affects catalytic efficiency, *e.g.* naringenin **3/13** *versus* eriodictyol **14** (Table 1)).

The absence of a 3′-hydroxyl group in the 2*S*-naringenin **3** substrate, compared to DHQ **9**, also causes an alteration in the hydrogen bonding between the B-ring of 2*S*-naringenin **3** with Tyr142 relative to the contacts between the B-ring of 2*R*,3*R*-*trans*-DHQ **9** and Tyr142. In the naringenin structure, there appears to be single hydrogen bond between Tyr142 and the 4′-hydroxyl group of 2*S*-naringenin **3**, whereas DHQ-1 **9** uses both its 3′- and 4′-hydroxyl to hydrogen bond to Tyr142. Further,

the position of the side chain of Y142 in the 2*S*-naringenin **3** structure is clearly defined and is rotated by *ca.* 14° relative to the DHQ **9** structure, bringing it closer to the naringenin substrate (if the A- and C-rings of 2*R*-naringenin **13** occupied the same position where 2*S*-naringenin **3** is modelled, there would be a distance of only 2 Å from the B-ring hydroxyl to $C_{\varepsilon 1}$ of Y142). The conformation of the side chain of Gln117 projects towards Tyr142, but it is too distant (3.7 Å) for a direct hydrogen bond to its phenolic oxygen. There is also an apparent rotation of V229, which is close to both the 2OG **1** and substrate binding sites.

ANS and flavonol synthase (FLS) mutants were designed based on potential involvement of amino acid side chains in acid–base catalysis during desaturation (ANS-K128A), binding of flavonoid substrates (ANS Y142H, ANS-K341H, K341N, FLS-H131Y and FLS-K329N) and binding of the MES molecule (ANS-E230Q, ANS-N131D, ANS-N131A), the latter of which had been postulated to be replacing L-ascorbic acid in the active site. ANS residue Y142 and the flavonol synthase residue H132 were targeted on the basis of crystallographic analyses, as the identity of the residues at this position represents a potential difference between the ANS and predicted flavonol synthase active sites. It was thought that these residues may be involved in determining substrate selectivity, so mutants in which the residues at position-142 for ANS (equivalent to position-128 for flavonol synthase) were interchanged were made (*i.e.* ANS-Y142H and FLS-H132Y).

The six ANS mutants (Y142H, E230Q, K128A, N131D, N131A, K341N) and two flavonol synthase mutants (H132Y and K329N) were prepared and purified (to >90% purity by SDS-PAGE analysis) as reported for the wild type enzymes, (ANS-E230Q bound less tightly to the Reactive Green column used for purification, but was obtained in a similar purity to the other mutants). Two other mutants, ANS-K213A and FLS-K202A, were produced in a predominantly insoluble form in *Escherichia coli* BL21(DE3) cells and were not pursued. ESI-MS analyses of the mutant proteins were all within 10Da (Table 4) of the calculated values and circular dichroism analyses indicated that they had similar folds to native ANS and flavonol synthase (data not shown).

The mutants were assayed by using HPLC to monitor for conversion of (±)-*trans*-DHQ (**9** and enantiomer) to quercetin **8**. All of the mutants displayed significant activity under standard assay conditions (Table 5). The K128A mutant was less active than wild type ANS (*ca.* 70% with (±)-*trans*-DHQ substrate) and when incubated with (±)-naringenin **3/13**, the relative amounts of apigenin **4** to dihydrokaempferol **5/10/11** produced remained reasonably consistent with that of the wild type. These results indicate that Lys128 is not essential for catalysis and specifically that it does not act as a general base during desaturation, at least under *in vitro* conditions. As mutation of Y142H in ANS did not increase the activity of ANS to that of flavonol synthase (Table 5) it can be concluded that the presence of the corresponding residue H132 in flavonol synthase is not solely responsible for the increased efficiency of flavonol synthase with 2*R*,3*R*-*trans*-DHQ **9** substrate. As for the wild type enzyme, optimal activity of all the mutants was dependent on L-ascorbic acid. Incubation with (±)-naringenin **3/13** demonstrated that all the mutants converted it to DHK **5/10/11**, apigenin **4** and kaempferol **12**.

Table 4 Masses of wild type and mutant enzymes

Enzyme	Predicted mass/Da	Experimental mass/Da
ANS wt	40 396	40 404 ± 14
ANS Y142H	40 343	40 348 ± 11
ANS K341N	40 382	40 378 ± 12
ANS E230Q	40 395	40 402 ± 15
ANS K128A	40 339	40 345 ± 6
ANS N131D	40 397	40 404 ± 8
ANS N131A	40 353	40 358 ± 6
FLS wt	38 281	38 284 ± 6
FLS H132Y	38 307	38 313 ± 7
FLS K329N	38 267	38 272 ± 5

Table 5 Relative activity of enzymes in comparison with wild types for assays with the (±)-*trans*-DHQ (**9** and enantiomer) substrate as determined by HPLC monitoring of quercetin **8** production. Figures are normalised to wild type enzymes (ANS or flavonol synthase). For flavonol synthase, figures in parentheses are normalised to those for ANS

Enzyme	Activity relative to wild type enzyme (%)
ANS wt	100.00
ANS Y142H	67.00
ANS K341N	70.00
ANS E230Q	48.00
ANS K128A	71.00
ANS N131D	82.00
ANS N131A	66.00
FLS wt	100 (224)
FLS H132Y	63 (140)
FLS K329N	28 (64)

Discussion

The work presented here is consistent with, and supports the proposal that ANS catalyses the oxidation of flavanone substrates (*e.g.* naringenin **3/13**) initially by removal of the C-3 *pro-S* hydrogen. At least for naringenin **3/13** and related substrates, the type of oxidation reaction catalysed, in particular hydroxylation *versus* desaturation, is dependent on the C-2 stereochemistry of the substrate. It seems likely that this influences the stereoelectronic relationship between the other reactive oxidising intermediate(s) and the naringenin substrate (**3** or **13**).

For some 2OG dependent oxygenases, including taurine dioxygenase and deacetoxycephalosporin C synthase, kinetic isotope studies are consistent with a mechanism in which a ferryl intermediate abstracts a hydrogen atom from the prime substrate.[25,26] This can be followed by substrate hydroxylation, desaturation or rearrangement. Desaturation can be envisaged to occur either by initial oxygenation followed by dehydration or *via* a more direct process not involving oxygenation (Fig. 12). In accord with an analogous radical rebound mechanism proposed for the ANS catalysed hydroxylation of naringenin **3/13** substrates, all the reactions may occur *via* formation of a common C-3 flavanone radical intermediate by removal of the C-3 *pro-S* hydrogen atom (Figs. 3 and 4).

For 2*S*-naringenin **3**, a single stereoisomer of *cis*-DHK **10** is produced as the major product (>70% of total detected flavanoid products), presumably 2*R*,3*S*-*cis*-DHK **10** (assuming retention of C-2 stereochemistry), formed by hydroxylation of the C-3 *pro-S* position (Fig. 3). This mechanism is supported by the ANS–Fe–2OG–naringenin–MES crystal structure (see below).

In contrast with 2*S*-naringenin **3**, in the case of 2*R*-naringenin **13** there is a significant decrease in the product (dia)stereoselectivity of hydroxylation (*i.e.* a *ca.* 1 : 1 ratio of *cis* : *trans* DHK was observed) coupled with a large increase in the relative amount of the direct desaturation product, apigenin **4** (Fig. 4).

ANS is proposed to catalyse the formal desaturation of 2*R*,3*R*-*trans*-DHQ **9** to give quercetin **8** *via* an oxygenating mechanism involving C-3 hydroxylation to give an enzyme bound geminal C-3,3-diol **15** intermediate, followed by dehydration (Fig. 2A).[23] ANS catalysed desaturation of some LCDs (*e.g.* 2*R*,3*S*,4*S*-*cis*-LCD **6**) may occur *via* an analogous process (Figs. 2B and 12), though for these substrates a mechanism proceeding *via* C-4 hydroxylation cannot be ruled out. However, it is unlikely that the apigenin **4** observed in the assay of 2*R*-naringenin **13** arises by an oxygenating hydroxylation followed by dehydration mechanism. This is because ANS is unable to

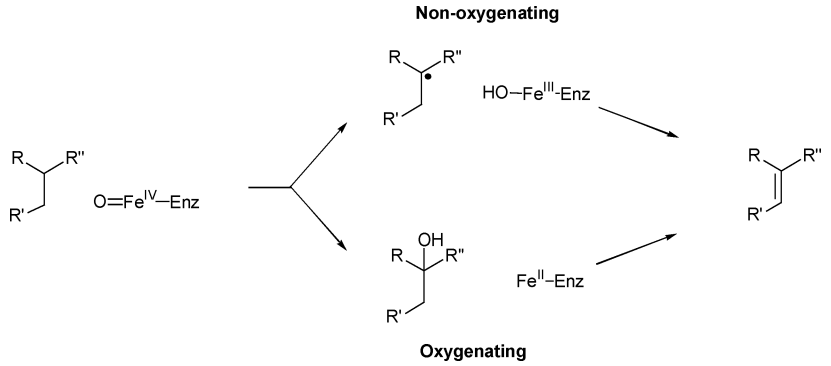

Fig. 12 Outline of possible non-oxygenating *versus* oxygenating mechanisms for desaturation. In the case of ANS, the oxygenation mechanism is proposed to occur when R″ = OH.

dehydrate dihydroflavonols (*i.e.* DHK **5** or DHQ **9**) to flavones (*i.e.* apigenin **4** and luteolin respectively), even when the former are formed in the active site, *e.g. cis*-DHQ is formed in the ANS active site in the reaction of 2*R*,3*S*,4*R*-*trans*-LCD substrates.[17] Thus, ANS catalysed C-2, C-3 desaturation of 2*R*-naringenin **13** to give apigenin **4** is likely to occur by removal of two hydrogen atoms by a reactive oxidising species, possibly without the direct aid of a catalytic base from an amino acid residue (Fig. 4). The mutagenesis studies are consistent with this proposal, as they rule out the critical involvement of residues including K128 of ANS, that could act as a general base.

For the 'direct' (compared to the hydroxylation–elimination reactions proposed for dihydroflavonols) desaturation reactions catalysed by non-haem Fe(II), 2OG dependent oxygenases, it has been suggested that following abstraction of the first hydrogen atom, the iron–oxygen derived species (probably Fe^{III}–OH) removes a second hydrogen atom from the substrate to generate a water molecule.[27] This process may either be concerted with desaturation, or proceeds *via* a radical species that collapses to form the product, after rearrangement in the case of some enzymes, *e.g.* deacetoxycephalosporin C synthase.

The proposed C-3 flavanone radical intermediate formed by removal of the C-3 *pro*-*S* hydrogen atom of 2*R*-naringenin **13** is a plausible intermediate in the formation of both 2*S*,3*S*-*trans*-DHK **11**, by α-face hydroxylation and apigenin **4**, by removal of the *syn*-facial C-2 hydrogen (Fig. 4). In comparison, a *syn*-facial desaturation mechanism involving the C-3 *pro*-*S* hydrogen of 2*S*-naringenin **3** cannot occur, consistent with the observation that only very low amounts of apigenin **4** are produced in incubations of ANS with 2*S*-naringenin **3**. These observations, together with prior work, demonstrate that C-3 oxidation on the α-face (equivalent to the *pro*-*S* C-3 hydrogen of naringenin **3**/**13**) is the predominant mechanism in ANS catalysis, but that in the case of the 2*R*-naringenin **13** substrate, β-face oxidation (hydroxylation) can also occur (Fig. 4).

Interestingly, the product stereoselectivity of hydroxylation at the C-3 position is reduced for incubations of 2*R*-naringenin **13** with ANS relative to that with 2*S*-naringenin **3**, possibly due to an alteration in the spatial arrangement between the ferryl (or equivalent) intermediate (Fig. 13) or an alternative fate for an intermediate involved in formation of the C-3 *pro*-*S* hydroxylated product.

The position of 2*S*-naringenin **3** in the active site relative to the iron in the ANS–Fe–2OG–naringenin–MES crystal structure supports the conclusions of the solution studies. The C-3 *pro*-*S* hydrogen is the most accessible to the iron centre and appears the most likely position for oxidation of both enantiomers of naringenin **3**/**13** by ANS. The structure of 2*S*-naringenin **3** bound to the active site shows that the C-2 hydrogen atom of 2*S*-flavanones (*e.g.* **3**) is likely to be inaccessible to oxidation. This is consistent with the low levels of apigenin **4** formed with this substrate and the proposal that apigenin **4** formation *in vitro* requires a *syn*-facial relationship between the C-2 hydrogen and the C-3 *pro*-*S* hydrogen, which is only possible with 2*R*-flavanones (*e.g.* **13**). Modelling 2*R*-naringenin **13** into the active site of ANS implied that the C-2 hydrogen is accessible for oxidation for this substrate (data not shown). However, the greater distance of the assumed position of the ferryl oxygen to the C-2 position of 2*R*-naringenin **13** compared to that of the C-3 position (*ca.* 6 Å and 5 Å, respectively) suggests that a concerted *syn*-facial C-2, C-3 mechanism is unlikely. As discussed above it seems more likely that a C-3 radical is initially formed by removal of the C-3 *pro*-*S* hydrogen of 2*R*-naringenin **13** prior to subsequent removal of its C-2 hydrogen and formation of apigenin **4** (Fig. 4).

In the ANS–Fe–2OG–DHQ_2 crystal structure, two molecules of DHQ (**9** and enantiomer) were observed to be bound to the active site; exposure of the crystals to dioxygen resulted in conversion of the DHQ **9** molecule closest to the iron centre to quercetin **8**, demonstrating that this complex is still catalytically active. However, it was not clear how the quercetin **8** product could exit the active site, without movement of the second molecule of DHQ (enantiomer of **9**). Although other explanations are possible, the observation of inhibition of ANS activity by high concentrations of flavonoid substrates is consistent with the catalysis being hindered by the formation of non-productive ANS–flavonoid complexes in which two molecules of flavonoid are bound at the active site.

In vitro assay results along with sequence similarities imply that flavone synthase I and flavanone 3β-hydroxylase (Fig. 1A) are predominantly β-face oxygenases (*i.e.* preferentially catalyse

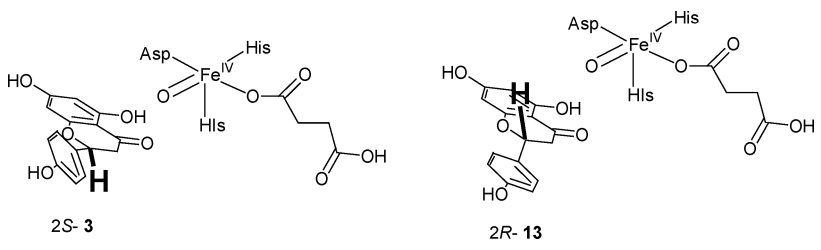

Fig. 13 Scheme outlining the possible position of the ferryl intermediate relative to the C-2 and C-3 hydrogen atoms of both 2*S*-**3** and 2*R*-naringenin **13** substrates. Note: the relative accessibility of the C-3 hydrogen in the latter case.

oxidation at the position equivalent to the C-3 *pro-R* hydrogen of naringenin **3/13**), while ANS and flavonol synthase are predominantly α-face oxygenases (the C-3 *pro-S* hydrogen atom of naringenin **3/13**).[23] In support of this proposal, the results presented here indicate that ANS can catalyse a *syn*-facial α-face desaturation. In comparison, the desaturation of 2*S*-naringenin **3** by flavone synthase I (Fig. 1A) is thought to occur by a *syn*-facial β-face mechanism.[4,15] The results also reveal that ANS *can* catalyse β-face oxidation, albeit as a minor pathway with the unnatural *R*-naringenin isomer-**13**, which gives 2*S*,3*R*-*cis*-DHK **10** as one of its products (Fig. 4).

There is current interest in the generation of synthetic catalysts based on the active sites of non-haem oxygenases.[10] Like the non-haem Fe(II), 2OG dependent oxygenases clavaminic acid synthase and deacetoxy/deacetylcephalosporin C synthase, ANS is able to catalyse more than one type of oxidative reaction, indicating the versatility of these catalysts. Studies on the 2OG oxygenase clavaminic acid synthase have shown that the balance between hydroxylation and desaturation can be affected by the nature of the substrate side chain.[21] In the case of ANS, the balance between hydroxylation and desaturation appears to be more subtle, being dependent on the stereochemistry at a single position. By choice of substrate stereochemistry it may be possible to use the same catalyst for both hydroxylation and desaturation reactions. The results demonstrate that ANS can catalyse formal desaturation by more than one type of mechanism: oxygenating or non-oxygenating. Thus, although the oxygenating mechanism is probably unusual, and proposed to proceed *via* a gem-diol intermediate then elimination of water, it should not be assumed that there is a unique desaturation mechanism for iron-dependent oxidising enzymes.

Materials and methods

ANS and flavonol synthase (*A. thaliana*) were over-expressed and purified according to published procedures.[23,28] General protocols, equipment and reagent sources were as reported.[23] The Stratagene QuikChange Site-Directed mutagenesis kit was used to create mutant pET-24a(+)-*ans* and pET-3a(+)-*fls* genes. The mutants were purified using the same procedure as for wild type ANS and flavonol synthase, except for ANS-E230Q which bound less tightly to the Reactive Green column. The mutations were confirmed by automated DNA sequencing carried out by the DNA Sequencing Service, Department of Biochemistry, University of Oxford.

The primers used for mutagenesis were as follows:

ANS Y142H:

Forward 5′-GTGGACAATTGGAATGGGAAGAT**C**ACTT-CTTTCATCTTGCGTATC-*3′*

Reverse 5′-CAGGATACGCAAGATGAAAGAAGT**G**ATC-TTCCCATTCCAATTGTC-*3′*

FLS H132Y:

Forward 5′-GCTTGGGTCGAT**T**ATCTCTTCCATCGAA-TCTGG-*3′*

Reverse 5′-GTGGCCAGATTCGATGGAAGAGAT**A**ATC-GACCC-*3′*

ANS K213A:

Forward 5′-GAGCTTCTTCTACAAATG**GC**GATAAATT-ACTATCCAAAATGTCCTCAGC-*3′*

Reverse 5′-GAGGACATTTTGGATAGTAATTTATC**GC**C-ATTTGTAGAAGAAGCTCTTC-*3′*

FLS K202A:

Forward 5′-GGCGGAGTATATGATG**GC**GATTAACTAT-TATCCGCCGTGTCC-*3′*

Reverse 5′-CACGGCGGATAATAGTTAATC**GC**CATCAT-ATACTCCGCCATC-*3′*

ANS E230Q:

Forward 5′-GCTAGCACTCGGTGTG**C**AAGCTCACAC-CG-*3′*

Reverse 5′-GTGAGCTA**G**CACACCGAGTGCTAGCTC-AG-*3′*

ANS K128A

Forward 5′-CAAGGCTATGGAAGT**GC**ATTGGCTAACA-ACGCGAG-*3′*

Reverse 5′-CCACTCGCGTTGTTAGCCAAT**GC**ACTTCC-ATCGCC-*3′*

ANS N131D:

Forward 5′-CAAGGCTATGGAAGTAAATTGGCT**G**ACA-ACGCGAG-*3′*

Reverse 5′-CCACTCGCGTTGT**C**AGCCAATTTACTTGC-ATAGCC-*3′*

ANS N131A:

Forward 5′-CAAGGCTATGGAAGTAAATTGGCT**GC**CA-ACGCGAG-*3′*

Reverse 5′-CCACTCGCGTTG**GC**AGCCAATTTACTTCC-ATAGCC-*3′*

ANS K341N:

Forward 5′-CAACATATTGAGCAT**GC**GTTGTTTGGGA-AGGAACAAGAAG-*3′*

Reverse 5′-CTTGTTCCTTCCCAAACAAC**GC**ATGCTCA-ATATGTTGAGC-*3′*

ANS K341A:

Forward 5′-CAACATATTGAGCAT**GC**GTTGTTTGGGA-AGGAACAAGAAG-*3′*

Reverse 5′-CTTGTTCCTTCCCAAACAAC**GC**ATGCTCA-ATATGTTGAGC-*3′*

FLS K329N:

Forward 5′-GGATTACAGTTACCGCAA**C**CTCAATAAA-CTTCCTCTGG-*3′*

Reverse 5′-GAGGAAGTTTATTGAG**G**TTGCGGTAACT-GTAATCCTTG-*3′*

FLS K329A:

Forward 5′-GGATTACAGTTACCGC**GC**GCTCAATAAA-CTTCCTCTGG-*3′*

Reverse 5′-GAGGAAGTTTATTGAGC**GC**GCGGTAACT-GTAATCCTTG-*3′*

Assay procedures

For the assays investigating the effect of different concentrations of (±)-naringenin **3/13** and (±)-*trans*-DHQ (**9** and enantiomer) on the initial rate of 2OG **1** decarboxylation, the method used was that of monitoring the decarboxylation of 1-[^{14}C]-2OG as described previously, except that assays were quenched after 1 min.[23]

HPLC assays were carried out and analysed as described previously,[23] except for those to separate *cis*-DHK **10** and *trans*-DHK **5/11** where the conditions were as follows. *Chiral HPLC analysis*—after SPE separation of the assay components, 200 μL of the 50% MeOH fraction were loaded at 0.8 mL min^{-1} onto a ChiraSpher® NT 250 × 4.6 column pre-equilibrated with 40% buffer A and 60% buffer B. The column was then run isocratically at 0.8 mL min^{-1} under similar solvent conditions.

The percentage yields were calculated by integration of peaks on HPLC traces. For assays of (±)-*trans*-DHQ (**9** and enantiomer) and (±)-naringenin **3/13** substrates, the elutant was monitored between 200 and 400 nm. For assays of LCD (*e.g.* **6**) substrates, the elutant was monitored between 200 and 600 nm. The HPLC system was calibrated for different flavonoid standards by 15 injections of known amounts of a compound giving an absorbance of <1.5 at the wavelength of interest. Using the equation area $= bx$, where x is the number of nmoles of compound and b is a conversion factor, the values calculated for b were cyanidin **7** (198 70828 at 520 nm), (±)-*trans*-DHQ (**9** and enantiomer) (180 32188 at 290 nm), quercetin **8** (172 92176 at 370 nm) and (±)-naringenin **3/13** (173 60805 at 290 nm). A standard of DHK **5/10/11** was not available in sufficient quantities for a calibration, so the same conversion factor was used as for naringenin **3/13** (which has a very similar chromophore).

Table 6 Data collection and refinement statistics for the ANS–Fe(II)–2OG–naringenin structure (PDB id code: 2brt)

Space group		$P2_12_12_1$
Resolution/Å		2.2 (2.31–2.2)
Unit cell/Å	*a*	56.8
	b	62.3
	c	102.5
Total reflections		109 275
Unique reflections		18 607
R_{merge}[a] (%)		0.082 (0.606)
Completeness (%)		98.0 (99.5)
I/σ_1		15.8 (3.1)
R		0.211
R_{free}		0.268
Mean B-values/Å^2		
Main chain		47.3
Side chain		48.0
Substrates		52.3
Iron		31.7
Solvent		47.8
RMS deviations from ideal		
Bonds/Å		0.025
Angles/°		1.89
No. solvent molecules		128

[a] $R_{merge} = \Sigma_j\Sigma_h|I_{h,j} - \langle I_h\rangle|/\Sigma_j\Sigma_h\langle I_h\rangle \times 100$ (outer resolution shell statistics shown in parentheses).

Substrate synthesis

2*R*-**13** and 2*S*-naringenin **3** were produced by naringinase mediated cleavage of the glycosidic bond of 2*R*- and 2*S*-naringin as described.[23]

^{1}H NMR scale naringenin incubations

Assays were carried out as 18 × 0.5 ml aliquots for 45 minutes, then combined and loaded onto an SPE column (Strata C-18E, 500 mg). The cofactors were eluted using 8 ml 5% MeOH (v/v); DHK **5/10/11** with 4 ml 40% MeOH (v/v); and naringenin **3/13** apigenin **4** with 60% MeOH (v/v). The ^{1}H NMR (500 MHz) spectra were assigned by comparison to standards (including doping experiments) and couplings confirmed by COSY spectra. For chiral ^{1}H NMR analyses, after the initial ^{1}H spectra had been recorded, Eu(hfc)$_3$-(+) was added portion wise (2 × 85 nmol, 1 × 170 nmol) from a 40 mM solution with a ^{1}H NMR spectrum recorded after each addition. Selected data as follows:

Naringenin **3/13**; δ_H (500 MHz; CD_3CN): 2.8 (dd, 1H, *J* 3.0 17.0, H-3), 3.1 (dd, 1H, *J* 13.0 17.0, H-3), 5.3 (dd, 1H, *J* 3.0 13.0, H-2), 5.8 (2d, 2H, *J* 2.1, H-6 H-8), 6.75 (d, 2H, *J* 8.5), 7.3 (d, 2H, *J* 8.5); λ_{max}: 291.4 nm; *m*/*z* (ESI-MS negative ion mode): $[M - H]^-$ 271.0.

Apigenin **4**; δ_H (500 MHz; CD_3CN): 6.3 (d, 1H, *J* 2.0), 6.55 (d, 1H, *J* 2.0), 6.65 (s, 1H, H-3), 7.0 (d, 2H, *J* 9.0), 8.0 (d, 2H, *J* 9.0); λ_{max}: 337.9 nm; *m*/*z* (ESI-MS negative ion mode): $[M - H]^-$ 269.0.

trans-DHK **5/11**; δ_H (500 MHz; CD_3CN): 4.6 (d, 1H, *J* 11.5, H-3), 5.0 (d, 1H, *J* 11.5 H-2); λ_{max}: 292.4 nm; *m*/*z* (ESI-MS negative ion mode): $[M - H]^-$ 287.0.

cis-DHK **10**; δ_H (500 MHz): 4.3 (d, 1H, *J* 3.0, H-3), 5.45 (d, 1H, *J* 3.0, H-2), 6.0 (2d, 2H, *J* 2.2, H-6 8), 6.85 (d, 2H, *J* 8.5), 7.35 (d, 2H, *J* 8.5); + 380 nmol Eu(hfc)$_3$-(+); δ_H (500 MHz): 11.75 (s, 1H); λ_{max}: 292.4 nm; *m*/*z* (ESI-MS negative ion mode): $[M - H]^-$ 287.0.

Eriodictyol **14** assay; *trans*-DHQ; *m*/*z* (ESI-MS negative ion mode): $[M - H]^-$ 303.0; λ_{max}: 290.2 nm. *cis*-DHQ; *m*/*z* (ESI-MS negative ion mode): $[M - H]^-$ 303.0; λ_{max}: 290.2 nm.

Crystals of (±)-naringenin **3/13** complexed with ANS–Fe(II)–2OG were grown from a solution of 18% (w/v) PEG 2000 monomethylether, 50 mM MES, 200 mM ammonium acetate, 2 mM $FeSO_4$, 10 mM potassium 2OG, 10 mM sodium ascorbate and 2.5 mM (±)-naringenin **3/13** (in MeOH to give a final concentration of 10% (v/v) MeOH), pH 6.5. The crystals were immersed in mother liquor supplemented with 10% (v/v) ethylene glycol and flash cooled in liquid N_2. Diffraction data were collected at 100 K using beamline 14.2 (SRS, Daresbury Laboratory, UK) with an ADSC Quantum4 CCD detector (Table 6). The data were processed using MOSFLM and SCALA (CCP4 suite[29]).

Acknowledgements

We thank the Biotechnology and Biological Sciences Research Council (Biomolecular Sciences Committee) and the Engineering and Physical Sciences Research Council for funding. We thank Dr J. L. Firmin (John Innes Centre, Norwich, UK) for providing the purified 2*S*- and 2*R*-naringin.

References

1 B. A. Bohm, *Introduction to Flavonoids*, Harwood Academic Publishers, Amsterdam, 1998.
2 G. Forkmann and W. Heller, *Comprehensive Natural Products Chemistry*, Elsevier Science, Amsterdam, 1999, pp. 713–748.
3 K. Springob, J. Nakajima, M. Yamazaki and K. Saito, *Nat. Prod. Rep.*, 2003, **20**, 288–303.
4 S. Martens, G. Forkmann, L. Britsch, F. Wellmann, U. Matern and R. Lukacin, *FEBS Lett.*, 2003, **544**, 93–8.
5 R. Lukacin, C. Urbanke, I. Groning and U. Matern, *FEBS Lett.*, 2000, **467**, 353–8.
6 A. G. Prescott, N. P. Stamford, G. Wheeler and J. L. Firmin, *Phytochemistry*, 2002, **60**, 589–93.
7 R. Lukacin, F. Wellmann, L. Britsch, S. Martens and U. Matern, *Phytochemistry*, 2003, **62**, 287–92.
8 K. Saito, M. Kobayashi, Z. Gong, Y. Tanaka and M. Yamazaki, *Plant J.*, 1999, **17**, 181–9.
9 J. J. Turnbull, W. J. Sobey, R. T. Aplin, A. Hassan, J. L. Firmin, C. J. Schofield and A. G. Prescott, *Chem. Commun.*, 2000, 2473–4.
10 M. Costas, M. P. Mehn, M. P. Jensen and L. Que, Jr., *Chem. Rev.*, 2004, **104**, 939–86.
11 R. P. Hausinger, *Crit. Rev. Biochem. Mol. Biol.*, 2004, **39**, 21–68.
12 J. C. Price, E. W. Barr, B. Tirupati, J. M. Bollinger, Jr. and C. Krebs, *Biochemistry*, 2003, **42**, 7497–508.
13 D. A. Proshlyakov, T. F. Henshaw, G. R. Monterosso, M. J. Ryle and R. P. Hausinger, *J. Am. Chem. Soc.*, 2004, **126**, 1022–3.
14 P. J. Riggs-Gelasco, J. C. Price, R. B. Guyer, J. H. Brehm, E. W. Barr, J. M. Bollinger, Jr. and C. Krebs, *J. Am. Chem. Soc.*, 2004, **126**, 8108–9.
15 L. Britsch, *Arch. Biochem. Biophys.*, 1990, **282**, 152–60.
16 R. W. D. Welford, J. J. Turnbull, T. D. W. Claridge, A. G. Prescott and C. J. Schofield, *Chem. Commun.*, 2001, 1828–9.
17 J. J. Turnbull, M. J. Nagle, J. F. Seibel, R. W. D. Welford, G. H. Grant and C. J. Schofield, *Bioorg. Med. Chem. Lett.*, 2003, **13**, 3853–7.
18 R. C. Wilmouth, J. J. Turnbull, R. W. D. Welford, I. J. Clifton, A. G. Prescott and C. J. Schofield, *Structure*, 2002, **10**, 93–103.
19 E. N. Marsh, M. D. Chang and C. A. Townsend, *Biochemistry*, 1992, **31**, 12648–57.
20 Z. H. Zhang, J. S. Ren, D. K. Stammers, J. E. Baldwin, K. Harlos and C. J. Schofield, *Nat. Struct. Biol.*, 2000, **7**, 127–33.
21 M. D. Lloyd, K. D. Merritt, V. Lee, T. J. Sewell, B. Wha-Son, J. E. Baldwin, C. J. Schofield, S. W. Elson, K. H. Baggaley and N. H. Nicholson, *Tetrahedron*, 1999, **55**, 10201–20.
22 J. E. Baldwin and M. Bradley, *Chem. Rev.*, 1990, **90**, 1079–88.
23 J. J. Turnbull, J. Nakajima, R. W. D. Welford, M. Yamazaki, K. Saito and C. J. Schofield, *J. Biol. Chem.*, 2004, **279**, 1206–16.
24 E. Kiehlmann and E. P. M. Li, *J. Nat. Prod.*, 1995, **58**, 450–5.
25 J. C. Price, E. W. Barr, T. E. Glass, C. Krebs and J. M. Bollinger, Jr., *J. Am. Chem. Soc.*, 2003, **125**, 13008–9.
26 J. E. Baldwin, R. M. Adlington, N. P. Crouch, J. W. Keeping, S. W. Leppard, J. Pitlik, C. J. Schofield, W. J. Sobey and M. E. Wood, *J. Chem. Soc., Chem. Commun.*, 1991, 768–70.
27 M. D. Lloyd, H. J. Lee, K. Harlos, Z. H. Zhang, J. E. Baldwin, C. J. Schofield, J. M. Charnock, C. D. Garner, T. Hara, A. C. T. van Scheltinga, K. Valegard, J. A. C. Viklund, J. Hajdu, I. Andersson, A. Danielsson and R. Bhikhabhai, *J. Mol. Biol.*, 1999, **287**, 943–60.
28 J. J. Turnbull, A. G. Prescott, C. J. Schofield and R. C. Wilmouth, *Acta Crystallogr., Sect. D: Biol. Crystallogr.*, 2001, **57**, 425–7.
29 Collaborative Computational Project Number 4, *Acta Crystallogr., Sect. D: Biol. Crystallogr.*, 1994, **50**, 760–763.